

NANO EXPRESS

Open Access

Enhanced functionalization of $\text{Mn}_2\text{O}_3@SiO_2$ core-shell nanostructures

Sonalika Vaidya, Pallavi Thaplyal, Ashok Kumar Ganguli*

Abstract

Core-shell nanostructures of $\text{Mn}_2\text{O}_3@SiO_2$, $\text{Mn}_2\text{O}_3@$ amino-functionalized silica, $\text{Mn}_2\text{O}_3@$ vinyl-functionalized silica, and $\text{Mn}_2\text{O}_3@$ allyl-functionalized silica were synthesized using the hydrolysis of the respective organosilane precursor over Mn_2O_3 nanoparticles dispersed using colloidal solutions of Tergitol and cyclohexane. The synthetic methodology used is an improvement over the commonly used post-grafting or co-condensation method as it ensures a high density of functional groups over the core-shell nanostructures. The high density of functional groups can be useful in immobilization of biomolecules and drugs and thus can be used in targeted drug delivery. The high density of functional groups can be used for extraction of elements present in trace amounts. These functionalized core-shell nanostructures were characterized using TEM, IR, and zeta potential studies. The zeta potential study shows that the hydrolysis of organosilane to form the shell results in more number of functional groups on it as compared to the shell formed using post-grafting method. The amino-functionalized core-shell nanostructures were used for the immobilization of glucose and L-methionine and were characterized by zeta potential studies.

Introduction

Surface modification is an integrated and crucial part of material processing and is the basis for the functionality of the material. These functional groups provide further accessibility for anchoring other substrates (or complexes), such as biomolecules or metal ions, into the pores and channels of the carrier material. Surface modification of materials started in early 1990. Badley et al. modified the surface of colloidal silica particles with mercaptopropyl, aminopropyl, and octadecyl chains. Since then modified silica nanoparticles have been utilized for various applications. Silica-coated magnetic nanoparticles modified with γ -mercaptopropyltrimethoxysilane (γ -MPTMS) have been used for solid phase extraction of trace amounts of Cd, Cu, Hg, and Pb [1]. Silanization of silica nanoparticles with 3-MPTMS and with N1-[3-(trimethoxysilyl)-propyl]diethylenetriamine has been developed and used for immobilization of oligonucleotides [2] and proteins [3]. Mesoporous vinyl silica was used for the immobilization of penicillin acylase which showed good initial enzymatic activity for the hydrolysis of penicillin G [4,5]. Yoshitake et al. [6] in their studies have shown

that the captured transition metal ions on amino-functionalized silica act as adsorption centers for arsenate ions. Surface-functionalized silica particles have found applications in catalysis [7-9], sensors [7,10], and protein immobilization [11,12]. Also, functional groups have been incorporated into silicate surfaces to facilitate molecular imprinting of those surfaces to form highly specific biomimetic catalytic or adsorbent materials [13-15]. Recently, ultrafine silica nanoparticles, with surfaces functionalized by cationic-amino groups, have been shown to not only bind and protect plasmid DNA from enzymatic digestion but also transfect cultured cells and express encoded proteins [16,17].

Two commonly applied methods for the introduction of functional groups onto the silica surface are co-condensation and post-grafting of functional silanes. Both the methods have certain drawbacks associated with them. The post-synthesis grafting method results in inhomogeneity of the functional group on the surface of the nanoparticles. This is because the organic moieties (functional groups) are concentrated near the entries of the mesopores and the exterior surfaces [18]. The second most commonly used for functionalization of nanoparticles is the co-hydrolysis of organosilanes with a tetraalkoxysilicate. Using the co-hydrolysis

* Correspondence: ashok@chemistry.iitd.ernet.in
Department of Chemistry, Indian Institute of Technology, Hauz Khas, New Delhi 110016, India

techniques, silica particles with surface vinyl [19,20], carboxylate [21], amine [22], dihydroimidazole [23], pyridine [15], and quaternary amine [15] have been developed. Co-condensation reactions of organotrialkoxysilanes and TEOS at various molar ratios were carried out by Mann and co-workers [24] to covalently link organo-functionalities such as phenyl, allyl, mercapto, amino, cyano, perfluoro, or dinitrophenylamino moieties to the core-shell nanostructures of Au coated with functionalized silica. However, the main disadvantage of this method is that most of the functional groups may be embedded in the silica network [25].

The above applications of modified silica particles motivated us to synthesize core-shell nanostructures of Mn_2O_3 nanoparticles (core) with functionalized silica shell. Silica-coated Mn_2O_3 (not functionalized) nanostructures were also synthesized. Mn_2O_3 is an antiferromagnetic oxide with the transition temperature of 90 K. It is used as a catalyst in the oxidation of ethylene [26] and methane [27] and in the decomposition of NO_x [28]. Nanocomposites of Mn_2O_3 and Mn_3O_4 on mesoporous silica showed significant catalytic activity toward CO oxidation below 523 K [29]. The oxidative dehydrogenation of ethane in wet natural gas over Mn_2O_3/SiO_2 catalyst was investigated by Ping et al. [30]. In most of the earlier reports the functionalizing agent is assembled after the formation of the silica shell, or a co-condensation method has been used. In our studies we have optimized the conditions such that the functionalized shell can be formed from the hydrolysis of the respective precursors, i.e., the organotrialkoxysilanes to form amino-, allyl-, and vinyl-functionalized silica shell. To the best of our knowledge there has been only one report on the formation of amino-functionalized silica shell over ultrasmall superparamagnetic iron oxide particles (USPIO) using the hydrolysis of the organosilane. These particles were coated with silica, (3-aminopropyl) trimethoxysilane (3-APTMS), and [*N*-(2-aminoethyl)-3-aminopropyl]trimethoxysilane (AEAPTMS), and their ability to label immortalize progenitor cells for magnetic resonance imaging (MRI) was compared. It was observed that the three coated USPIO particles were biocompatible and were intensely internalized in immortalized progenitor cells which make them a suitable candidate for MR cell-labeling and cell-tracking experiments [31]. Thus, we believe that our methodology will ensure more functional groups over the core-shell nanostructures and hence can be used for biological applications in a more efficient way. In this study we also show the ability of these nanostructures to immobilize glucose and L-methionine.

Our methodology, using surfactant, can be used to synthesize silica shell over nanoparticles which are synthesized at high temperature and are not present in

colloidal form (have high degree of agglomeration). Our study can also be extended to form silica shell over individual nanoparticles (having high degree of agglomeration) which can then be used in various biomedical and catalytic applications. We have also increased the concentration of functional groups on the surface of core-shell nanostructures with the use of organosilane precursors to form the shells. The methodology is an improvement over the commonly used post-grafting or co-condensation method. This point has been proved in this article by carrying out two studies: one with zeta potential and other using a fluorescamine dye. Thus, the methodology described can be used to synthesize core-shell nanostructures with *high density of functional groups* which can be further used for various analytical purposes such as extraction of trace elements with high specificity. The high density of functional groups will also ensure an increase in the number biomolecules or drugs that can be immobilized on these nanostructures. For this we have carried out a case study using glucose and L-methionine and have shown that the functionalized core-shell nanostructures can be used to immobilize biomolecules.

Materials and methods

Mn_2O_3 nanoparticles were synthesized by thermal decomposition of manganese oxalate nanorods [32]. For the synthesis of core-shell nanostructures with silica shell, Mn_2O_3 nanoparticles were dispersed in Tergitol/cyclohexane mixture. Silica coating was carried out using hydrolysis of TEOS with ammonia. Amino-functionalized core-shell nanostructures Mn_2O_3 nanoparticles were dispersed in Tergitol/1-octanol/cyclohexane mixture followed by hydrolysis of 3-APTMS using ammonia and water. Vinyl- and allyl-functionalized core-shell nanostructures were synthesized by dispersing Mn_2O_3 nanoparticles in Tergitol/water system. The functionalized silica shell was grown over the Mn_2O_3 nanoparticles by hydrolysis of vinyltrimethoxysilane and allyltrimethoxysilane using ammonia. In order to confirm that the above methodology ensures more functional groups on the core-shell, Mn_2O_3 @amino-functionalized silica core-shell nanostructures were also synthesized by the post-grafting method wherein Mn_2O_3 nanoparticles were dispersed in Tergitol/1-octanol/cyclohexane mixture. Mn_2O_3 nanoparticles were coated with silica using TEOS as the shell forming agent followed by addition of 3-APTMS. Amount of amino groups on the core-shell nanostructures with amino-functionalized silica (with and without TEOS) was calculated using fluorescamine dye.

Glucose and L-methionine immobilization was carried out by taking amino-functionalized core-shell nanostructures in phosphate buffer (pH 8) to form a dispersion

under sonication. To this, glucose solution was added followed by stirring for 48 h for the immobilization of glucose while L-methionine immobilization was carried out by addition of L-methionine solution followed by stirring for 24 h after which the resultant mixture was heated at 60°C. The above core-shell nanostructures were characterized using powder X-ray diffraction (PXRD), FTIR, HRTEM, surface charge measurement (zeta potential), and fluorescence studies. All the details regarding synthesis and characterization are given in the supporting information.

Results and discussion

TEM image of $\text{Mn}_2\text{O}_3@\text{SiO}_2$ core-shell nanostructures shows cores with size ranging from 25 to 100 nm with a shell thickness of 5 nm (Figure 1a). The presence of amorphous silica shell was clearly observed in the TEM image. The synthetic methodology utilizes already synthesized Mn_2O_3 nanoparticles which has been prepared from the route known in the literature [32]. HRTEM image (Figure 1b) shows lattice fringes corresponding to (111) plane of Mn_2O_3 . The amorphous silica shell was clearly observed surrounding the crystalline core in the high resolution TEM image (Figure 1b). Thus HRTEM of $\text{Mn}_2\text{O}_3@\text{SiO}_2$ core-shell nanostructures confirms the chemical composition of core as Mn_2O_3 and shell as amorphous silica.

$\text{Mn}_2\text{O}_3@\text{SiO}_2$ core-shell nanostructures are present in an aggregated form as observed from TEM images in Figure 1. The presence of aggregates could be attributed to the formation of H-bond between the silica shells due to the presence of Si-OH bond over the shell surface. These Si-OH bonds were formed by the hydrolysis of TEOS in the presence of ammonia and water at room temperature. We have also discussed the aggregation effect in silica-coated core-shell nanostructures in our earlier report [33]. It is also to be noted that the starting material (Mn_2O_3 nanoparticles) used for the synthesis of silica shell is a magnetic material, present in powder form. Thus, there is an inherent tendency of these oxide nanoparticles to agglomerate. However, a challenge still remains to form silica shell over individual nanoparticles (for the oxides present in powder form with high degree of agglomeration). The main emphasis in this article is on the enhancement of functional groups on the surface of core-shell nanostructures by using an organosilane precursor to form the shell and compared with our studies of shell formation by the post-grafting method which has been the common procedure in earlier studies [25]. This point has been discussed in later sections.

Figure 2a shows TEM image for Mn_2O_3 @amino-functionalized silica particles with core diameter of 25-30 nm and shell thickness of 5 nm. Nanoparticles of

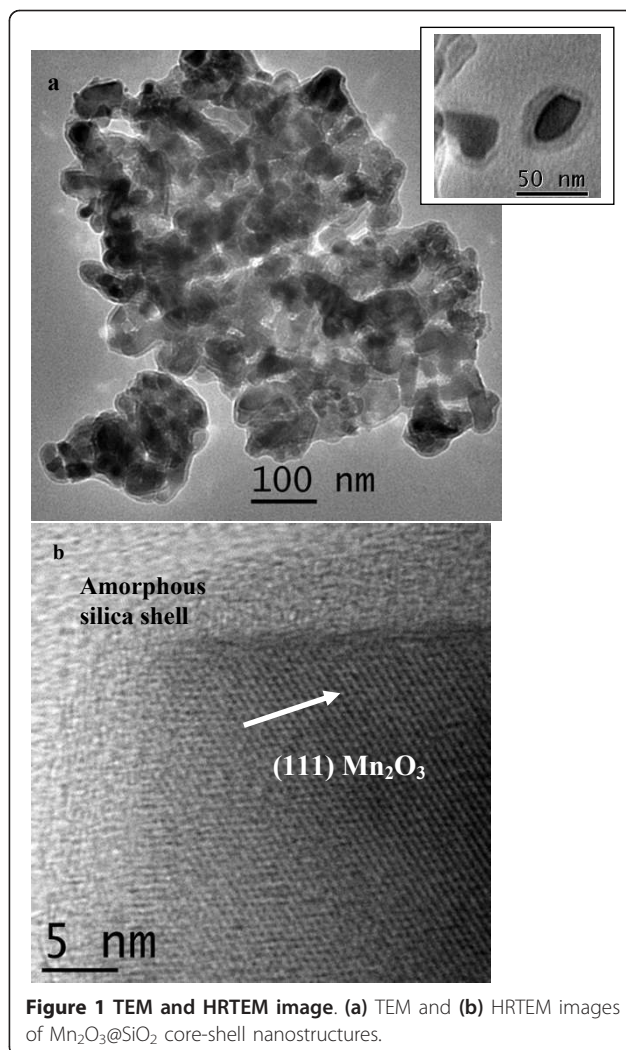
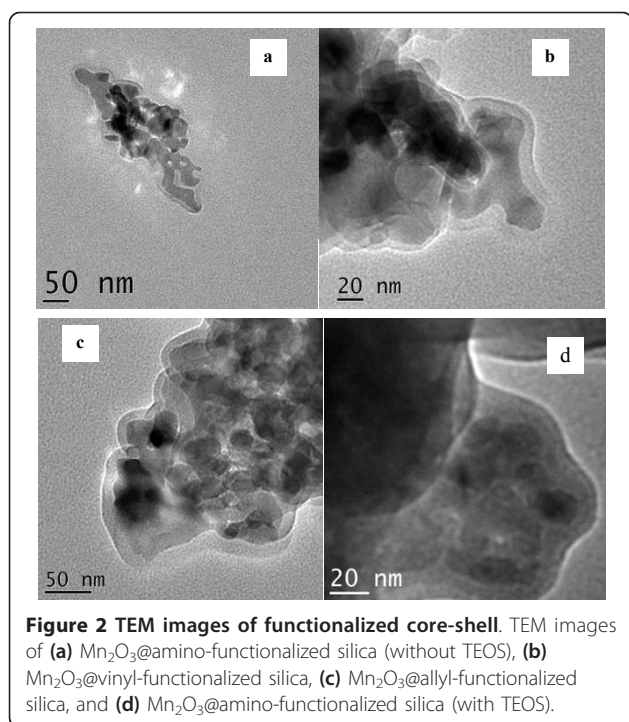


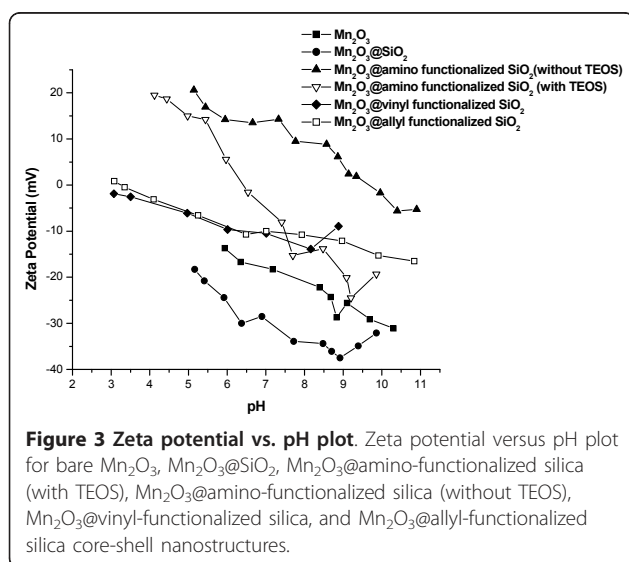
Figure 1 TEM and HRTEM image. (a) TEM and (b) HRTEM images of $\text{Mn}_2\text{O}_3@\text{SiO}_2$ core-shell nanostructures.

Mn_2O_3 @vinyl-functionalized silica (Figure 2b) show core-shell nanostructures with a core diameter of 25-30 nm and shell thickness of 5-10 nm. Cores with diameter of 25-30 nm with a shell thickness of 10-15 nm were observed (Figure 2c) for Mn_2O_3 @allyl-functionalized silica. It is to be noted that the shell in the above three core-shell nanostructures is formed by the hydrolysis of organosilane precursors, which ensures that these core-shell nanostructures bear the respective functional groups (amine, vinyl, and allyl) on their surface. Core-shell nanostructures (amine groups over the shell) were obtained (Figure 2d) when the synthesis was carried out with TEOS and APTMS. The core size varied from 20 to 25 nm and a shell thickness was found to be 10 nm.

Bands at 3429, 1632, 572, and 520 cm^{-1} corresponding to O-H stretching, O-H bending, and Mn-O stretching were observed in IR spectrum of Mn_2O_3 nanoparticles. Additional bands at 1123 and 1079 cm^{-1} corresponding to Si-O-Si stretching were observed for the silica-coated



nanostructures. This gives further evidence for the coating of silica over Mn_2O_3 nanoparticles corroborating with the TEM studies. Table S1 in Additional file 1 summarizes the IR bands for the functionalized core-shell nanostructures. Note that in all the three core-shell nanostructures, Si-O-Si stretching band was observed even though TEOS was not added. This confirms that the stretching band was observed due to the functionalized silica shell formed as a result of hydrolysis of the organosilane precursors. Thus, IR spectrum gives us an additional proof for the formation of core-shell nanostructures with functionalized shells. In



addition to the above we also observed C=C stretching vibrations in the IR spectrum of vinyl- and allyl-functionalized core-shell nanostructures which also suggest the proper functionalization of the shell.

Zeta potential studies for uncoated and coated Mn_2O_3 nanoparticles were carried out with varying pH (Figure 3). Increase in the negative zeta potential values were observed for the coated particles compared to the uncoated particles, which suggests a uniform coating of silica over Mn_2O_3 nanoparticles. The negative surface charge of silica is expected due to the presence of hydroxyl groups on the surface of silica.

Figure 3 shows zeta potential versus pH curves for bare Mn_2O_3 , Mn_2O_3 @ SiO_2 , Mn_2O_3 @amino-functionalized silica (with TEOS), Mn_2O_3 @amino-functionalized silica (without TEOS), Mn_2O_3 @vinyl-functionalized silica, and Mn_2O_3 @allyl-functionalized silica core-shell nanostructures. The silica-coated Mn_2O_3 bears a negative surface charge at $\text{pH} > 3$. It has been reported in an earlier study [34] that the presence of amine shifts the iso-electric point (IEP) toward higher pH values as the pK_a of aminopropyl group is 9.8. The amine group is protonated at $\text{pH} < 9$. In Mn_2O_3 @amino-functionalized silica (without TEOS), the IEP was found to be 9.6 which suggests that the amino groups are present on the surface of the core-shell particles. At $\text{pH} > \text{IEP}$, deprotonation of the positively charged R-NH_3^+ groups results in a negative surface charge while the presence of R-NH_3^+ groups at $\text{pH} < \text{IEP}$ results in a positive surface charge. The zeta potential depends on two main factors viz. pH and concentration of the sample [35]. In our study we have fixed the concentration of the sample from 1 to 2 mg in 10 ml of 10 mM NaCl and have studied the zeta potential as a function of pH.

Zeta potential values are sensitive to the surface charge of the outer particle surface and hence our result suggests that the amine groups are located on the outer surface of the core-shell nanostructures. It is also to be noted that the values of the obtained zeta potential do not refer to a single particle but represent an ensemble of particles present in the system. In order to ensure that more functional groups are present over the shell, zeta potential studies were carried out on Mn_2O_3 @amino-functionalized silica (with TEOS) wherein amino functionalization was carried out by post-grafting method using APTMS. It was observed that the zeta values were less positive than Mn_2O_3 @amino-functionalized silica (without TEOS). Zeta values as earlier mentioned are dependent on the surface charge of the outer particle, which suggests that the number of amine groups over the functionalized core-shell nanostructures synthesized using post-grafting method is less than the one synthesized using APTMS as the shell forming agent. The IEP for Mn_2O_3 @amino-functionalized silica (with TEOS) also shifts to low pH (=6.3), which also

suggests the presence of less number of amine groups and more number of hydroxyl groups over the surface of these core-shell nanostructures. The above inference was further confirmed by using fluorescamine dye. The concentration of amine groups was found to be 0.302 $\mu\text{mol/g}$ in the case of Mn_2O_3 @amino-functionalized silica (without TEOS) and 0.274 $\mu\text{mol/g}$ for Mn_2O_3 @amino-functionalized silica (with TEOS).

Surface charge density was calculated using Guoy-Chapman equation [36]. The surface charge density was calculated at two pH value viz. 5.4 and 6.5 and was found to be 3.96 mC/m^2 (at pH 5.4) and 3.14 mC/m^2 (at pH 6.5) for Mn_2O_3 @amino-functionalized silica (without TEOS). The surface charge density for Mn_2O_3 @amino-functionalized silica (with TEOS) was found to be 3.31 mC/m^2 (at pH 5.4) and -0.37 mC/m^2 . Thus, both calculations (using fluorescamine and zeta potential) suggest that the core-shell nanostructures (amino-functionalized) synthesized using the hydrolysis of 3-APTMS only bear high density of amino groups on the shell as compared to the core-shell nanostructures synthesized using post-grafting method.

The zeta potential of allyl- and vinyl-functionalized silica was higher than that of silica-coated and bare nanoparticles, which also suggests the presence of allyl and vinyl groups on the surface of the core-shell nanostructures.

Zeta potential studies for the amino-functionalized core-shell nanostructures immobilized with glucose and L-methionine were carried out by dispersing the particles in 10 mM NaCl solution (Table 1). The zeta potential values changed from positive to negative suggesting that glucose and L-methionine have been immobilized onto the surface of the core-shell nanostructures. Thus, the change in zeta potential values can be used to detect the immobilization of bio-molecules over nanoparticles. The immobilization of biomolecules (glucose and L-methionine) is just to show the use of functionalized silica core-shell structures for possible applications.

Conclusions

Synthesis of core-shell nanostructures with functionalized silica shell was carried out using the hydrolysis of the organosilane precursors. TEM shows the formation

Table 1 Zeta potential values for amino-functionalized and bio-molecule immobilized core-shell nanostructures

| Sample | Zeta potential (mV) |
|---|---------------------|
| Mn_2O_3 @amino-functionalized SiO_2 | 29.5 |
| Glucose immobilized Mn_2O_3 @amino-functionalized SiO_2 | -7.2 |
| L-methionine immobilized Mn_2O_3 @amino-functionalized SiO_2 | -12.0 |

of core-shell with a core diameter of 25-30 nm and a shell nanostructures thickness of 5-15 nm. An increase in (negative) the zeta potential value compared to the bare Mn_2O_3 and silica-coated Mn_2O_3 core-shell nanostructures also confirms the presence of functional groups over the surface of the core-shell. We have also shown that the hydrolysis of the organosilane precursor results in increased value of the zeta potential and the surface charge density, which confirms more number of functional group over the nanostructures.

Additional material

Additional file 1: Supplemental Material. A description of the experimental methods, supplementary figures and tables. **Figure S1. The PXRD pattern of Mn_2O_3 @ SiO_2 core-shell nanostructures.** Reflections corresponding to Mn_2O_3 (cubic) with a broad feature in the 2 theta range from 20° to 30° are observed indicating the presence of amorphous silica coated on Mn_2O_3 particles. **Figure S2. EDAX spectrum of Mn_2O_3 @ SiO_2 core-shell nanostructures.** Figure shows peaks corresponding to Mn, O, and Si confirming their presence in the core-shell nanostructures. **Table S1 Details of the IR frequencies for functionalized core-shell nanostructures**

Abbreviations

AEAPTMS: [N-(2-aminoethyl)-3-aminopropyl]trimethoxysilane; 3-APTMS (3-aminopropyl)trimethoxysilane; IEP: iso-electric point; γ -MPTMS: γ -mercaptopropyltrimethoxysilane; MRI: magnetic resonance imaging; USPIO: ultrasmall superparamagnetic iron oxide particles.

Acknowledgements

AKG thanks the NSTI, Department of Science & Technology, and CSIR, Govt. of India for financial support. SV thanks CSIR, Govt. of India for a fellowship.

Authors' contributions

SV carried out the synthesis and characterization of core-shell nanostructures. PT assisted in the synthesis of core-shell nanostructures. Basic idea and the execution of the project was carried out under the guidance of AKG. All authors read and approved the final manuscript.

Competing interests

The authors declare that they have no competing interests.

Received: 25 May 2010 Accepted: 24 February 2011

Published: 24 February 2011

References

- Huang C, Hu Bi: Silica-coated magnetic nanoparticles modified with γ -mercaptopropyltrimethoxysilane for fast and selective solid phase extraction of trace amounts of Cd, Cu, Hg, and Pb in environmental and biological samples prior to their determination by inductively coupled plasma mass spectrometry. *Spectrochimica Acta Part B* 2008, **63**:437-444.
- Hilliard L, Zhao X, Tan W: Immobilization of oligonucleotides onto silica nanoparticles for DNA hybridization studies. *Anal Chimica Acta* 2002, **470**:51-56.
- Qhobosheane M, Santra S, Zhang P, Tan W: Biochemically functionalized silica nanoparticles. *Analyst* 2001, **126**:1274-1278.
- Chong ASM, Zhao XS: Functionalized nanoporous silicas for the immobilization of penicillin acylase. *Appl Surf Sci* 2004, **237**:398-404.
- Chong ASM, Zhao XS: Design of large-pore mesoporous materials for immobilization of penicillin G acylase biocatalyst. *Catal Today* 2004, **93-95**:293-299.
- Yoshitake H, Yokoi T, Tatsumi T: Adsorption Behavior of Arsenate at Transition Metal Cations Captured by Amino-Functionalized Mesoporous Silicas. *Chem Mater* 2003, **15**:1713-1721.

7. Schubert U, Husing N, Lorenz A: **Hybrid Inorganic-Organic Materials by Sol-Gel Processing of Organofunctional Metal Alkoxides.** *Chem Mater* 1995, **7**:2010-2027.
8. Schubert U: **Catalysts made of organic-inorganic hybrid materials.** *New J Chem* 1994, **18**:1049-1058.
9. Kriesel JW, Tilley TD: **Synthesis and chemical functionalization of high surface area dendrimer-based xerogels and their use as new catalyst supports.** *Chem Mater* 2000, **12**:1171-1179.
10. Lev O, Tsionsky M, Rabinovich L, Glezer V, Sampal S, Pankaravot I, Gun J: **Organically modified sol-gel sensors.** *Anal Chem* 1995, **67**:22A-30A.
11. Kallury KM, Lee WE, Thompson M: **Enhanced stability of urease immobilized onto phospholipid covalently bound to silica, tungsten and fluoropolymer surfaces.** *Anal Chem* 1993, **65**:2459-2467.
12. Esker AR, Brode PF, Rubingh DN, Rauch DS, Yu H, Gast AP, Robertson CR, Trigiante G: **Protease Activity on an Immobilized Substrate Modified by Polymers: Subtilisin BPN'.** *Langmuir* 2000, **16**:2198-2206.
13. Markowitz MA, Kust PR, Deng G, Schoen PE, Dordick JS, Clark DS, Gaber BP: **Catalytic Silica Particles via Template-Directed Molecular Imprinting.** *Langmuir* 2000, **16**:17591765.
14. Sasaki DY, Alam TM: **Solid-State ³¹P NMR Study of Phosphonate Binding Sites in Guanidine-Functionalized, Molecular Imprinted Silica Xerogels.** *Chem Mater* 2000, **12**:1400-1407.
15. Markowitz MA, Deng G, Gaber BP: **Effects of Added Organosilanes on the Formation and Adsorption Properties of Silicates Surface-Imprinted with an Organophosphonate.** *Langmuir* 2000, **16**:6148-6155.
16. He XX, Wang K, Tan W, Liu B, Lin X, He C, Li D, Huang S, Li J: **Bioconjugated Nanoparticles for DNA Protection from Cleavage.** *J Am Chem Soc* 2003, **125**:7168-7169.
17. Roy I, Ohulchanskyy TY, Bharali DJ, Pudavar HE, Mistrtra RA, Kaur N, Prasad PN: **Optical tracking of organically modified silica nanoparticles as DNA carriers: A nonviral, nanomedicine approach for gene delivery.** *Proc Natl Acad Sci USA* 2005, **102**:279-284.
18. Kickelbick G: **Hybrid Inorganic-Organic Mesoporous Materials.** *Angew Chem Int Ed* 2004, **43**:3102-3104.
19. Espiard P, Mark JE, Guyot A: **A novel technique for preparing organophilic silica by water-in-oil microemulsions.** *Polym Bull* 1990, **24**:173-179.
20. Marini M, Pourabbas B, Pilati F, Fabbri P: **Functionally modified core-shell silica nanoparticles by one-pot synthesis.** *Colloid Surf A: Physicochem Eng Aspects* 2008, **317**:473-481.
21. Izutsu H, Mizukami F, Sashida T, Maeda K, Kiyozumi Y, Akiyama Y: **Effect of malic acid on structure of silicon alkoxide derived silica.** *J Non Cryst Solids* 1997, **212**:40-48.
22. Oh C, Lee J-H, Lee Y-G, Lee Y-H, Kimb J-W, Kang H-H, Oh S-G: **New approach to the immobilization of glucose oxidase on non-porous silica microspheres functionalized by (3-aminopropyl)trimethoxysilane (APTMS).** *Colloid Surf B: Biointerfaces* 2006, **53**:225-232.
23. Markowitz MA, Schoen PE, Kust P, Gaber BP: **Surface acidity and basicity of functionalized silica particles.** *Colloid Surf A: Physicochem Eng Aspects* 1999, **150**:85-94.
24. Hall SR, Davis SA, Mann S: **Co condensation of Organosilica Hybrid Shells on Nanoparticle Templates: A Direct Synthetic Route to Functionalized Core-Shell Colloids.** *Langmuir* 2000, **16**:1454-1456.
25. Calvo A, Joselevich M, Soler-Illia GJAA, Williams FJ: **Chemical reactivity of amino-functionalized mesoporous silica thin films obtained by co-condensation and post-grafting routes.** *Micropor Mesopor Mater* 121:67-72.
26. Dmuhovskiy B, Freerks MC, Zienty FB: **Metal oxide activities in the oxidation of ethylene.** *J Catal* 1965, **4**:577-580.
27. Anderson RB, Stein KC, Feenan JJ, Hofer LJE: **Catalytic Oxidation of Methane.** *J Ind Eng Chem* 1961, **5**:809-812.
28. Yamashita T, Vannice A: **Temperature-programmed desorption of NO adsorbed on Mn₂O₃ and Mn₃O₄.** *Appl Catal B: Environ* 1997, **13**:141-155.
29. Han Y-F, Chen F, Zhong Z, Ramesh K, Chen L, Widjaja E: **Controlled Synthesis, Characterization, and Catalytic Properties of Mn₂O₃ and Mn₃O₄ Nanoparticles Supported on Mesoporous Silica SBA-15.** *J Phys Chem B* 2006, **110**:24450-24456.
30. Lu P, Lu S-J, Qiu F-L: **Activation of ethane in wet natural gas over a Mn₂O₃/SiO₂ catalyst.** *J Nat Gas Chem* 1999, **8**:68-75.
31. Zhang C, Wängler B, Morgenstern B, Zentgraf H, Eisenhut M, Untenecker H, Krüger R, Huss R, Seliger C, Semmler W, Kiessling F: **Silica- and Alkoxy silane-Coated Ultrasmall Superparamagnetic Iron Oxide Particles: A Promising Tool To Label Cells for Magnetic Resonance Imaging.** *Langmuir* 2007, **23**:1427-1434.
32. Ahmad T, Ramanujachary KV, Lofland SE, Ganguli AK: **Nanorods of manganese oxalate: a single source precursor to different manganese oxide nanoparticles (MnO, Mn₂O₃, Mn₃O₄).** *J Mater Chem* 2004, **14**:3406-3410.
33. Vaidya S, Ramanujachary KV, Lofland SE, Ganguli AK: **Synthesis of homogeneous NiO@SiO₂ core-shell nanostructures and the effect of shell thickness on the magnetic properties.** *Cryst Growth Des* 2009, **9**:1666-1670.
34. Rosenholm JM, Lindén M: **Wet-Chemical Analysis of Surface Concentration of Accessible Groups on Different Amino-Functionalized Mesoporous SBA-15 Silicas.** *Chem Mater* 2007, **19**:5023-5034.
35. Medrzycka KB: **The effect of particle concentration on zeta potential in extremely dilute solutions.** *Colloid Polym Sci* 1991, **269**:85-90.
36. Obi I, Ichikawa Y, Kakutani T, Senda M: **Electrophoresis, Zeta potential and Surface Charges of Barley Mesophyll Protoplasts.** *Plant Cell Physiol* 1989, **30**:129-135.

doi:10.1186/1556-276X-6-169

Cite this article as: Vaidya et al.: Enhanced functionalization of Mn₂O₃@SiO₂ core-shell nanostructures. *Nanoscale Research Letters* 2011 **6**:169.

Submit your manuscript to a SpringerOpen® journal and benefit from:

- Convenient online submission
- Rigorous peer review
- Immediate publication on acceptance
- Open access: articles freely available online
- High visibility within the field
- Retaining the copyright to your article

Submit your next manuscript at ► springeropen.com